

Surface Analysis of Poly(ether urethane) Blending Stearyl Poly(ethylene oxide) Coupling Polymer

Dong-an Wang, Jian Ji, and Lin-Xian Feng*

Department of Polymer Science and Engineering, Zhejiang University, Hangzhou, 310027, P.R. China

Received August 19, 1999; Revised Manuscript Received December 1, 1999

ABSTRACT: A coupling polymer, abbreviated SPEO-MDI-SPEO (MSPEO), was synthesized by a simple reaction between 4,4'-methylenediphenyl diisocyanate (MDI) and stearyl poly(ethylene oxide) (SPEO, M_n 1900), and the blended poly(ether urethane) (PEU) films of PEU-MSPEO were prepared by a solution process. According to the analysis of ATR-FTIR, it was proved that when MSPEO was blended into the PEU matrix, the middle blocks (M-block) of MSPEO could incorporate with the hard blocks of PEU chains through the linkage of a H bond, leading to the improvement in the blending stability. The surface modification was finally accomplished by the self-motion of MSPEO since the elastomeric property of the matrix permits the modifiers to move freely. In the case of air, due to the relatively poor compatibility and rather low surface energy of the stearyl end groups, they migrated to the polymer–air interface, and thus the connected PEO chains were also enriched there by the tow of the end groups. However, in the case of water, the hydrophilic PEO chains migrated to the outermost layer of the surface, and finally they were enriched on the polymer–water interface, while the hydrophobic stearyl end groups would bend down back into the surface. Therefore, a PEO chain-loop structure was finally formed. Furthermore, also based on the mechanism of self-motivated surface modification, even if a part of MSPEO on the surface would have been washed away by water, the continuous makeup from the bulk would still be able to maintain the quantity of the PEO chains on the interface for a long time. All the results were verified by ^1H NMR, ATR-FTIR, XPS, and contact angle measurements.

Introduction

Poly(ether urethanes) (PEU) have been widely used in biomedical applications because of their fairly good tissue compatibility and excellent mechanical properties.¹ However, they are known to induce thrombogenic reactions when in contact with blood.^{2–4} It is believed that the blood coagulation on the foreign materials, also including the potential inflammatory reactions, is controlled by the proteins that are adsorbed or attached to these surfaces.^{5,6} Poly(ethylene oxide) (PEO) has been extensively considered as an effective surface-modifying additive (SMA) due to its ability to resist protein adhesion. Stearyl poly(ethylene oxide) (SPEO) is a derivative type of PEO with a stearyl group (C_{18}) at one of the double PEO chain ends. The C_{18} contained surface can differentially identify and adsorb the albumin in human plasma, which can passivate the surface and minimize the thrombogenic activations.^{7–9} A number of useful monographs on similar surface modifications with these classes of materials have been published.^{10–13}

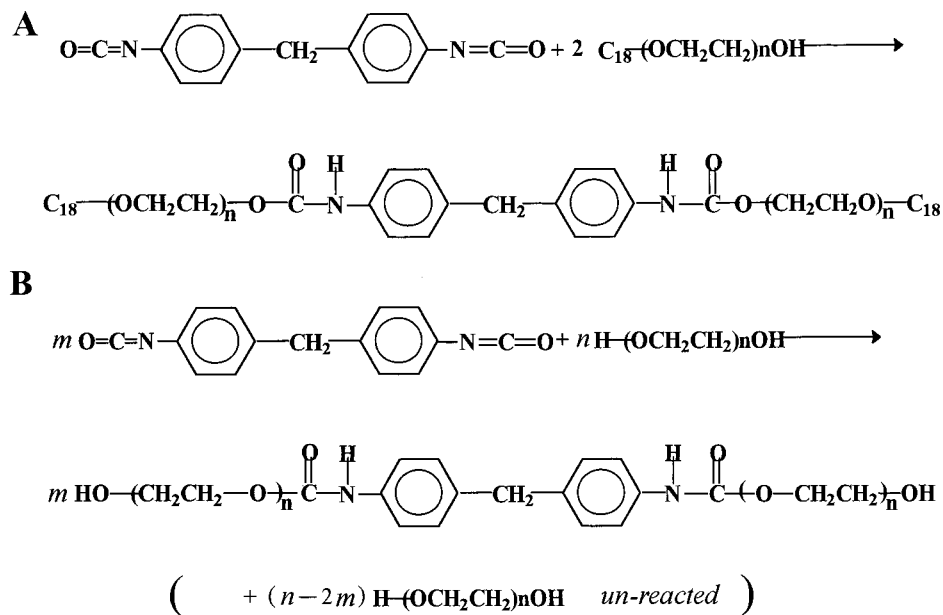
PEO can be incorporated into the surface of a polymeric matrix using the physical solution method. A process named surface physical interpenetrating network (SPIN)¹⁴ had been developed by several investigators. This blend system in surface layer has been proved to be kinetically stable for a variety of matrices, such as poly(ethylene terephthalate) (PET).¹⁵ Nevertheless, PEU is an elastomer at room temperature, and PEO chains can move freely within this matrix. Therefore, they can be lost away quickly under an aqueous circumstance. And due to the incompatibility of PEO with PEU, this process is further accelerated by the phase separation. So far, the unstability of the PEO–PEU blend system in an aqueous environment is still an unsolved problem.

To enhance the stability of PEU blends, the interaction between SMA and PEU matrix must be strengthened. It is well-known that the polymeric chains of PEU are composed of polyether “soft” blocks and aromatic urethane “hard” blocks alternatively. Within the bulk of PEU, the polymeric chains connect each other via H-bonds between hard blocks of the different chain segments, where the physical cross-linking points are formed and the strength of PEU material is yielded.¹ Starting from this point, we designed and synthesized a novel SMA, 4,4'-methylenediphenyl diisocyanate (MDI)–stearyl poly(ethylene oxide) (SPEO) coupling polymer (MSPEO). The coupling processes are schematically illustrated in Scheme 1. Besides MSPEO, a similar coupling polymer of PEO-MDI-PEO (MPEO) was also synthesized for comparison (see Scheme 1).

According to Scheme 1, the urethane block in the middle of MSPEO (M-block) has a very similar structure to the PEU hard block. When MSPEO is blended into the PEU matrix, H-bonds are also supposed to be formed between the M-blocks of MSPEO and the hard blocks of PEU chains. The blend system may therefore become much more stable. On the other hand, the SMAs will spontaneously migrate onto surface of matrix due to the incompatibility of MSPEO with PEU matrix. The surface modification was thus finally accomplished through this SMA's self-motivated surface enrichment besides the enhancement in blending stability by H-bonds. The performances and surface structures of the blends of PEU-MSPEO, PEU-MPEO, and PEU-SPEO have been studied in this paper.

Experimental Section

Materials and Synthesis. MDI (Yixing Chemical Factory, China) was purified using vacuum distillation. SPEO and PEO (Hangzhou Electrochemical Factory, China, M_n of SPEO 1900,

Scheme 1. Preparation of the MSPEO Coupling Polymer (A) and Preparation of the MPEO Coupling-Polymer (B)^a

^a The value of n/m was selected as 10 and 2, respectively, where the $\text{C}_{18,s}$ indicate the stearyl groups.

M_n of PEO 2000) were purified by dissolving in CHCl_3 and precipitating with ethyl ether. The solvent butanone was dried by distilling. As an initiator, di-*n*-butyltin dilaurate (DBTDL) was used without further purification. MSPEO or MPEO was prepared by a simple coupling reaction between isocyanate and polyether. The preparation route is illustrated in Scheme 1. However, the products with a broad distribution were always yielded during the synthesis of MPEO as the molar ratio of PEO/MDI, n/m in Scheme 1B, was 2. Therefore, PEO was far overdosed up to $n/m = 10$ in order to reduce the byproducts. The unreacted (S)PEO was finally removed by fractional precipitation with ethyl ether. The products were characterized by GPC, ^1H NMR, and FTIR.

Biomedical grade PEU pellets (for short PEL, Pellethane 2363-80AE) used in this study were supplied by Dow Chemical, Midland, MI. The blended films of PEL-MSPEO, PEL-MPEO, and PEL-SPEO with the thickness of 100–200 μm (measured with vernier caliper) were prepared using the technology reported by Bengt et al.¹⁶ The percentage of SMA added was 5% (w/w). The films were characterized by ^1H NMR, XPS, ATR-FTIR, and contact angle measurements (sessile drop method).

Leaching Experiment. The leaching processes were performed in an isothermal water bath. The stability of PEL-MSPEO was evaluated by two methods. (i) The films were immersed in daily refreshed water at 37 and 70 $^\circ\text{C}$ for 7 days. (ii) The films were incubated in toluene at room temperature for 60 h, followed by incubation in water at 37 $^\circ\text{C}$ for 24 h. The samples of PEL-SPEO were only leached in the second way.

GPC. GPC (Baseline 810 method, Waters) with an ultraviolet detector (Waters 486, UV) and a refraction index detector (R401 DET, nl-n0, RI) was used to verify the synthesis and the purification of M(S)PEO. The UV detector can differentially identify the π -conjugated structures, such as that on M-blocks.

^1H NMR. ^1H NMR spectroscopy (500 MHz, AVANCE DMX500, Bruker) was employed to detect the composition of the blends in D-DMSO (Aldrich).

ATR-FTIR. ATR-FTIR (E.S.P., MAGNA-IR560, Nicolet) was used to glean the qualitative and semiquantitative information including band assignments of different moieties and the formation of H-bonding within a depth of 400 nm from the air–polymer interface or the water–polymer interface.^{17,18} For measurement of the water–polymer interface, the samples were first immersed in water for 24 h and then examined after a quick vacuum-dry at room temperature.

XPS. As a complementary method of ATR-FTIR surface analysis, X-ray photoelectron spectroscopy was recorded on VG Instruments. The takeoff angle (θ) of 0° was selected for the maximal depth of approximately 10 nm.

Contact Angle Measurements. Contact angles were measured on a JY-82 goniometer. After the polymer films were cast on ultraclean stainless steel plates, all samples were extracted with water for 90 h and then dried thoroughly and quickly. The sessile method was performed. With the syringe, drops ($\leq 0.5 \mu\text{L}$) of deionized water were positioned onto the polymer surfaces. All the data of contact angle were read from the scale on the lens of the microscope at the 15th second after the water dropping.

Results and Discussion

GPC. The reactions of MDI with SPEO or PEO were monitored by GPC. RI and UV detectors were applied for measurements. Since the unreacted (S)PEO has no π -conjugated groups, it is not UV-sensitive. The GPC curves of resulted products are shown in Figure 1. For the reaction between MDI and SPEO, the components of the final product are respectively the desired MSPEO and the unreacted reactants. The pure MSPEO was obtained after fractional precipitation from raw product with ethyl ether, which was confirmed by Figure 1a. The situation for the reaction between MDI and PEO was more complicated. Within the final obtained mixture, besides the desired MPEO and unreacted reactants, the byproducts of PEO-MDI “AB” alternative copolymer with a variety of repeated units might be also present. When the ratio PEO/MDI of 2 was used, it can be seen from Figure 1b that the raw product had a broad distribution. To enhance the yield of the desired MPEO, more PEO, the ratio PEO/MDI of 10, was used, and the byproducts were effectively avoided. After removing unreacted PEO by fractional precipitation with ethyl ether, MPEO with high purity was obtained, which can be confirmed by Figure 1c.

^1H NMR. The analysis of ^1H NMR was performed for the detection of PEO. The spectra of the synthesized products and PEL-MSPEO blended film are shown in Figure 2. Through the blending process, the component

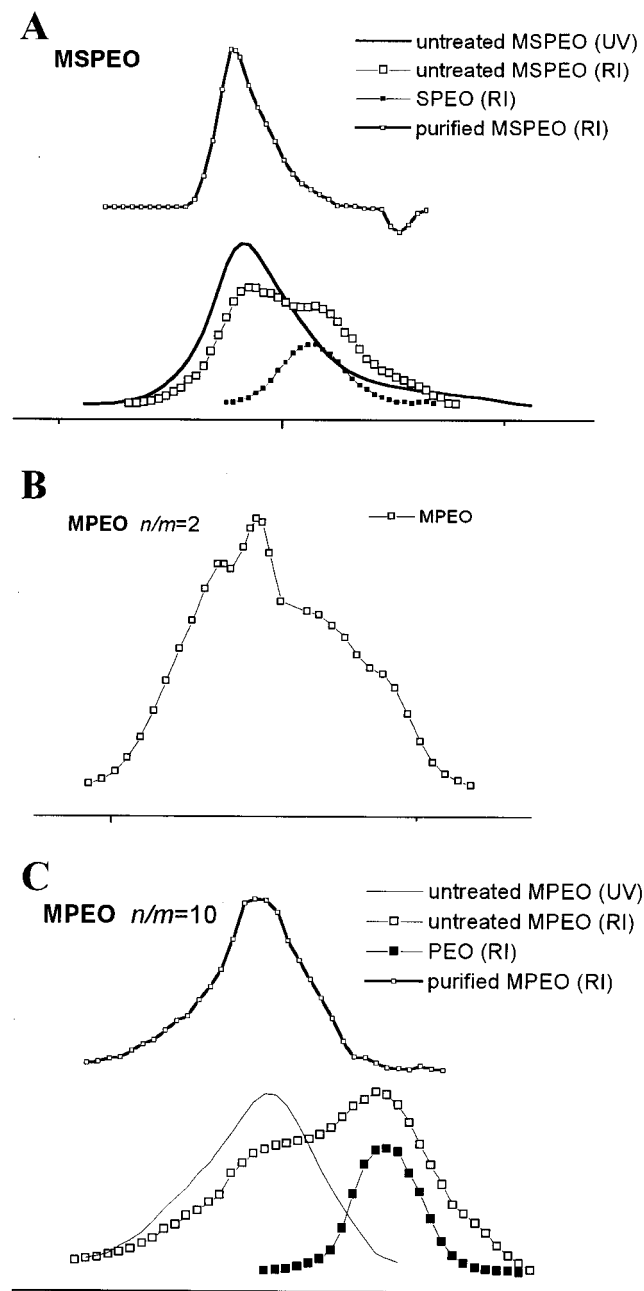


Figure 1. Gel permeation chromatography for the products of MDI-(S)PEO: (A) chromatography of MSPEO examined by RI and UV detectors, material SPEO by RI detector; (B) chromatography of MPEO ($n/m = 2$, n/m is the ratio of PEO/MDI, mol/mol, when the synthesis of MPEO) examined by RI detectors; (C) chromatography of products, MPEO ($n/m = 10$)-examined by RI and UV detectors, the material PEO by RI detector.

of EO, $\delta = 3.52$ ppm, was introduced into the blend system.

The data of leaching experiments according to the normalized variation of the integral EO hydrogen peak area are given in Table 1. The results of method i indicated that when the temperature was above the T_m of PEO (66°C),¹⁹ the blend system had poor stability, while under the physiological conditions, the blending stability was fairly good. The results of both method i and method ii could illuminate the effect of M-block's presence on the improvement of blending stability.

ATR-FTIR. ATR-FTIR is one of the most useful methods to detect the surface composition, from which

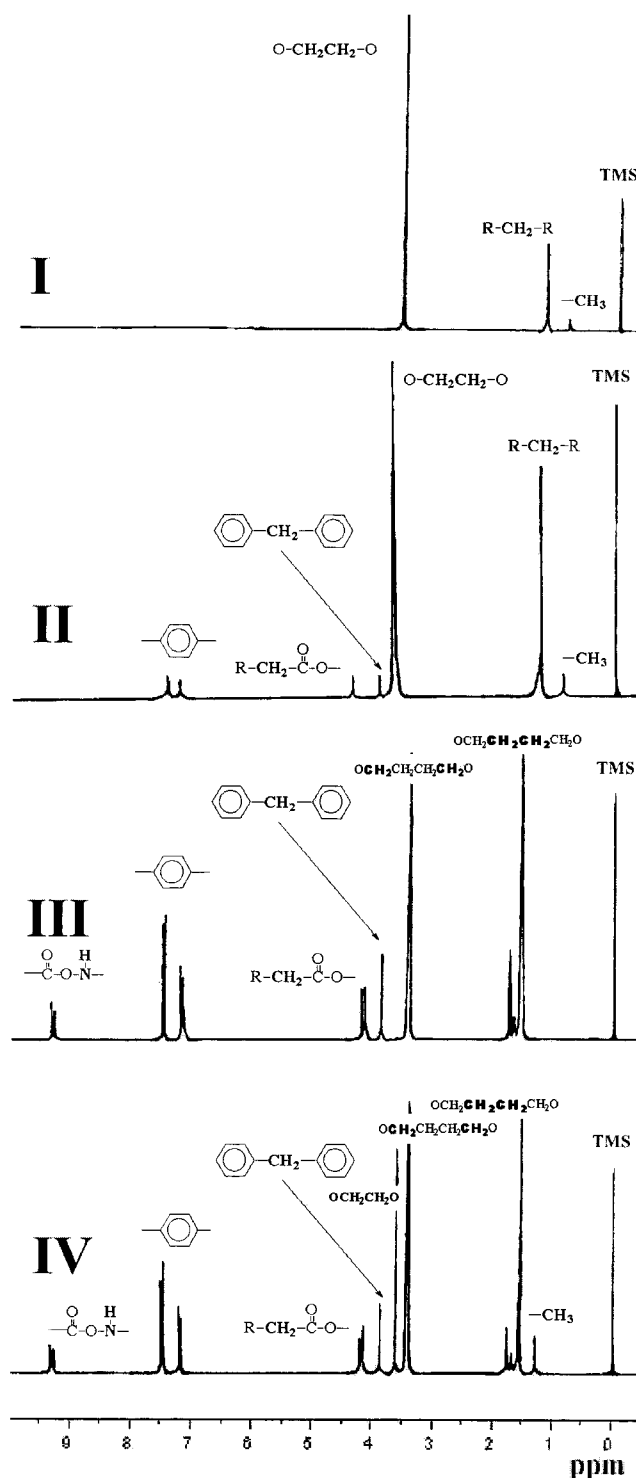


Figure 2. ^1H NMR spectra: I, SPEO; II, MSPEO; III, PEL; IV, PEL-MSPEO.

Table 1. Percentage of EO Loss after Leaching

method	conditions	% of EO loss (normalized from ^1H NMR data)	
		PEL-SPEO	PEL-MSPEO
(i)	water leaching, 37°C	68	15
	water leaching, 70°C	99	90
(ii)	toluene leaching, 37°C	99	60

the surface structure or conformation can be interpreted. The spectra for samples are shown in Figure 3. From each of the spectra, four key peaks were quantified according to the theory of Lambert-Beer, and four

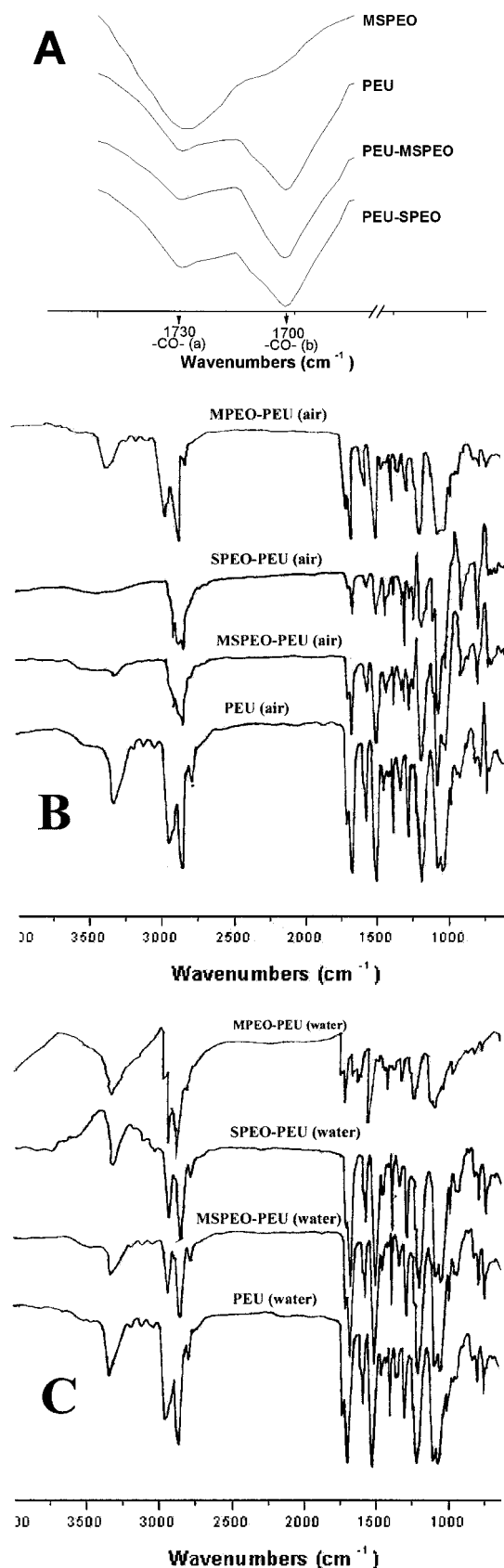


Figure 3. Spectra of ATR-FTIR: (A) 1745–1685 cm^{-1} : MSPEO, PEL, PEL-MSPEO, PEL-SPEO; (B) PEL, PEL-SPEO, PEL-MSPEO, PEL-MPEO, respectively, on the air interface; (C) PEL, PEL-SPEO, PEL-MSPEO, PEL-MPEO, respectively, on the water interface. Those spectra for the samples on water interface were given after 24 h immersing, followed by a quick vacuum-dry at room temperature, and then examined within a short time.

Table 2. Data of ATR-FTIR Analysis by Lambert-Beer's Law

ratio of groups	PEL	PEL-SPEO	PEL-MSPEO	PEL-MPEO
(i) Data for Air-Matrix Interface				
-CO- (b)/ -CO- (a)	1.807	1.857	2.000	
-O-/-CH ₂ -	1.174	4.063	2.368	
-CH ₂ -/-CO- (b)	0.835	2.462	0.950	1.120
-O-/-CO- (b)	0.981	4.927	2.250	0.920
(ii) Data for Water-Matrix Interface				
-CO- (b)/ -CO- (a)	1.839	1.833	2.000	
-O-/-CH ₂ -	0.918	1.462	1.843	
-CH ₂ -/-CO- (b)	0.933	0.675	0.571	2.455
-O-/-CO- (b)	0.856	0.987	1.054	1.182

corresponding ratios were given. In Lambert-Beer's formula,

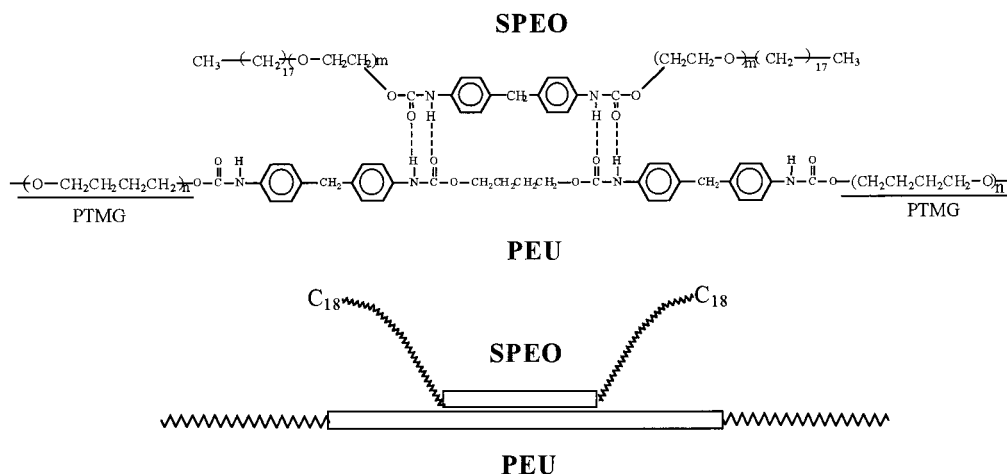
$$\lg \frac{I_0}{I_0 - H} = kcl$$

I_0 is the intensity of the incidence, H is the value of peak height, c is the concentration of the concerned component, l is the thickness of the tested sample, and k is a constant. Since all the samples were tested on the same spectrophotometer and all the samples had the same matrix PEL, the parameter l could be considered as another constant. Therefore, the value of $\lg[I_0/(I_0 - H)]$ is in proportion to the concentration of the concerned group, and the ratios of the same certain two peaks from different spectra are comparable. This is the basis of the semiquantification.

The four selected peaks were -CH₂- at 2853 cm^{-1} , free -CO- (a) at 1730 cm^{-1} , H-bonded -CO- (b), with -NH-)²⁰ at 1700 cm^{-1} , and -O- at 1105 cm^{-1} . The four corresponding ratios were -O-/-CH₂-, -CO- (b)/-CO- (a), -CH₂-/-CO- (b), and -O-/-CO- (b). Through the semiquantitative analysis, two basic questions would be discussed. The first one was the property of the linkage between the MSPEO and the matrix PEL. The second one was about the surface enrichment of PEO, as well as the surface structure and conformation, on both polymer-air interface and polymer-water interfaces. Finally, the models of the various interfaces would be given. Data of the ratios are shown in Table 2.

About H-Bond. As reported in refs 20 and 21, the assignment of the infrared H-bonding band in polyurethanes is mainly performed in the -CO- stretching regions. The band of free carbonyl groups, -CO- (a), was approximately at 1730 cm^{-1} , and the band of H-bonded (with -NH-) carbonyl groups, -CO- (b), was approximately at 1700 cm^{-1} . As shown in Figure 4, the ratio of -CO- (b)/-CO- (a) in MSPEO was rather low, indicating that most of the carbonyl groups of MSPEO were -CO- (a), and few H-bonds were formed among the MSPEO molecules. On the contrary, the carbonyl groups of PEL were mainly composed of H-bonded -CO- (b). In PEL-MSPEO, the ratio of -CO- (b)/-CO- (a) was further enhanced. Thus, the conclusion can be deduced: in the surface layer of PEL-MSPEO the interaction between the SMA-MSPEO and the matrix PEL was based on the H-bonds between the M-blocks of MSPEO and the hard blocks of PEU chains, which could be described in Scheme 2.

About Surface Enrichment of PEO. The groups of -CH₂- and -O- in PEL are mainly located on the soft blocks of PTMG [poly(tetramethylene glycol)], and

Scheme 2. Incorporation of the M-Block of MSPEO with Hard Block of PEU Chain by the Linkage of H-Bonds^a


^a The long and short bars indicate the hard blocks of PEU chain and M-block of MSPEO, respectively, the thin wave lines indicate the PEO chains of MSPEO, the wide wave lines indicate the PTMG (polytetramethylene glycol) chains of PEU, the C₁₈'s indicate the stearyl groups, and the dashed straight lines indicate the H-Bonds.

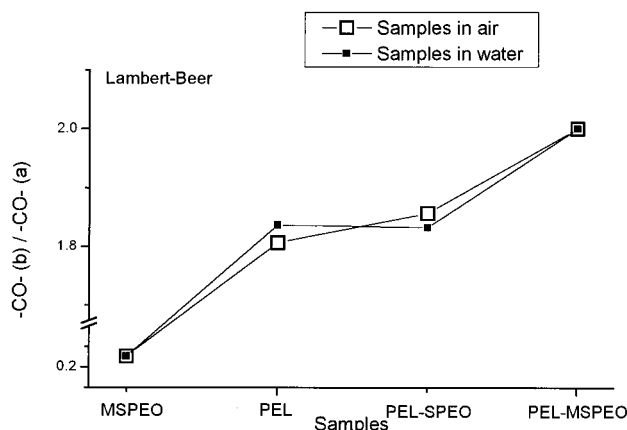


Figure 4. ATR-FTIR data ratios of the H-bonded carbonyl groups, $-\text{CO}-$ (b) to the free carbonyl groups $-\text{CO}-$ (a) on the air interface and water interface. The samples are MSPEO, PEL, PEL-MPEO, and PEL-MSPEO.

in MSPEO they are on the chains of PEO as well as a part of $-\text{CH}_2-$, on the C₁₈ end groups. For PTMG the value of $-\text{O}-/-\text{CH}_2-$ is 1/4, and for SPEO it is approximately 1/2. Because of this difference, the PEO chains' enrichment in the surface layer can be detected. As seen in Table 2, compared with that of PEL, both on the air-polymer interface and on the water-polymer interface, the $-\text{O}-/-\text{CH}_2-$ ratios on PEL-SPEO and PEL-MSPEO surfaces were remarkably increased, which could imply the enrichment of SPEO chains.

About Surface Structure and Conformation. To obtain further results, the ratios of $-\text{CH}_2-/-\text{CO}-$ (b) and $-\text{O}-/-\text{CO}-$ (b) were also given in Table 2. The $-\text{CH}_2-/-\text{CO}-$ (b) ratios can mainly illuminate the enrichment of PEO chains and the C₁₈ groups. The $-\text{O}-/-\text{CO}-$ (b) ratios can just illuminate the case of the PEO chains.

On the air interface, as shown in Table 2, the $-\text{O}-$ groups were dramatically enriched on the surface of PEL-SPEO; on the PEL-MSPEO surface, the enrichment was obvious but not so dramatic; and on the PEL-MPEO surface, the enrichment of $-\text{O}-$ was hardly observable. At the same time, the $-\text{CH}_2-$ groups were also dramatically enriched on the surface of PEL-SPEO, but on the PEL-MSPEO or PEL-MPEO surface the

enrichment was not obvious. Since the surface accumulation of PEO chains will only lead to the elevation of the ratios of $-\text{O}-/-\text{CH}_2-$ and $-\text{O}-/-\text{CO}-$ (b), the increase of $-\text{CH}_2-/-\text{CO}-$ (b) on the surface of PEL-SPEO should be explained as the enrichment of C₁₈ groups and/or PEO chains' oversaturated accumulation.

Because of rather low surface energy and poor compatibility with the matrix, the C₁₈ groups would migrated to the air-polymer interface, by the tow of which the PEO chains that were also incompatible with the matrix would be enriched there accordingly. This is the mechanism of the outward self-motivated surface modification on the air interface. For MSPEO or MPEO which had been physically cross-linked on the PEU chains by H-bonds, the whole activity was limited, so that the enrichment was relatively weak, especially for MPEO which contained no C₁₈, one of the main driving factors.

On the water interface, the $-\text{O}-$ groups were remarkably enriched on the surface of PEL-MPEO, while the enrichment was relatively weak on the PEL-MSPEO or PEL-SPEO surface. For the $-\text{CH}_2-$ groups, they were only dramatically enriched on the surface of PEL-MPEO, and no enrichment was observed on the PEL-MSPEO or PEL-MPEO surface. However, from the enrichment of $-\text{O}-$ and also from the results of $-\text{O}-/-\text{CH}_2-$, the PEO chains' surface enrichment was confirmed to be always in existence for both PEL-SPEO and PEL-MSPEO, whether on the air interface or on the water interface. Then the explanation was that for MSPEO or SPEO, due to the repulsion of water, their hydrophobic C₁₈ end groups would leave the water-polymer interface and return into the surface layer. Therefore, for PEL-SPEO, the SPEO chains in the surface layer would reverse the orientation of themselves due to the coeffect of the hydrophilic PEO chain segments and the hydrophobic C₁₈ end groups (seen in Scheme 3D,E). For PEL-MSPEO whose M-blocks of MSPEO were fixed on the hard blocks of the matrix PEU chains through H-bonds, the hydrophobic C₁₈ end groups would bend down and the hydrophilic PEO chains would stretch out. Then the situation would be like that the two ends of each PEO chain stayed below the outermost surface layer, but the body of the chain was stretched above the water-matrix interface. There-

Table 3. Data of XPS Analysis for the Samples

peak no.	peak area	block [%]
(1) Data of Untreated PEL (Seen in Figure 5b)		
C1 1s	46.465	
C2 1s	27.055	91.017
C3 1s	51.582	
C4 1s	9.958	7.245
C5 1s	0.189	1.739
C6 1s	2.201	
(2) Data of PEL-MSPEO (Seen in Figure 5c)		
C1 1s	19.808	
C2 1s	13.522	47.510
C3 1s	24.674	
C4 1s	62.281	51.011
C5 1s	0.883	1.479
C6 1s	0.922 18	

Table 4. Data of the Contact Angle Measurement for the Modified Samples

sample	contact angle (deg)
PEL (pure)	30.50 ± 2.5
PEL-MSPEO (SPIN) ^a	17.9 ± 2.6
PEL-MSPEO (blending)	5.20 ± 1.4
PEL (pure) reported ^b	35.2 ± 2.7
PEL-PEO 18.5K (SPIN) reported ^b	24.6 ± 4.3

^a This datum was from the job of our Lab. ^b The "values reported" were reported by Desai et al.¹⁵

binding energy value of each peak has no exact physical meaning. The assignments of the C 1s peaks are given in Figure 5, and the data of peak area are listed in Table 3. Through semiquantitative analysis, the results could be given. Compared with the pure PEL film, in the spectrum of PEL-MSPEO the normalized intensity of the C 1s peak for C–O increased dramatically. Furthermore, the value of O/C in the survey spectrum also increased from 0.2091 to 0.2788. All these indicated that for PEL-MSPEO, even after 7 days water leaching at 37 °C, there were still a great number of PEO chains enriched within the depth of 10 nm from the interface. Therefore, MSPEO's surface enrichment could be confirmed.

As mentioned above, after having been leached by water at 37 °C, the content of MSPEO in the whole bulk was 15% reduced, which was determined by ¹H NMR. Here, according to the result of XPS, it could be concluded that even if a part of MSPEO on the surface had been washed away by water, the continuous makeup from the bulk would still be able to maintain the quantity of the PEO chains on the interface for a long time, which was based on the mechanism of self-motivated surface modification.

Contact Angle Measurements. The data of contact angles are shown in Table 4. The decrease of the contact angle indicates the increased hydrophilicity of the polymer surfaces. The results of pure PEL and PEL-MSPEO (SPIN) were quite close to the reported data.¹⁵ However, the contact angle of the PEL-MSPEO was much smaller than others, meaning that its hydrophilicity was further enhanced and the hydrophilic PEO must be enriched on the water–polymer interface. On the other hand, since the end groups, C₁₈, of MSPEO was highly hydrophobic, the decrease of the contact angle indicated that the C₁₈'s were not on the water–polymer interface. This agrees with the PEO chain-loop's model structure on the water interface. The reason why the surface hydrophilicity of MSPEO (blending) was improved much more than that of PEL-MSPEO (SPIN) was probably the larger density of the SMA's surface enrichment.

Conclusions

As described above, a novel SMA for blood compatibility, MSPEO, was successfully synthesized and introduced into the surface of PEU materials through a simple blending process. With surface analysis by ATR-FTIR, XPS, and contact angle measurements, it was confirmed that the linkage between the matrix PEU chains and MSPEO was due to H-bonds. Furthermore, a relatively long time enrichment of the SMA was verified, and the models of the conformation on both air–polymer interface and water–polymer interface were also given. Thereinto, a special PEO-chain-loop structure was formed on the water interface of the PEL-MSPEO blended film.

After the leaching experiment, the blended components were detected by ¹H NMR in the bulk and by XPS in the surface layer. The results indicated that, based on the blending mechanism of H-bond, the stability of the system was enhanced. Moreover, it was observed that even if there would be a certain loss on the gross of the SMA in the bulk, the quantity of SMA on the surface would hardly decrease, which was really essential to surface modification. The reason for this phenomenon, as well as for the final accomplishment of the surface modification, lies in the self-motivated mechanism of MSPEO's surface enrichment.

Acknowledgment. This research was financially supported by NSFC (No. 29804009) and the Chinese National Ministry of Education.

References and Notes

- (1) Lelah, M. D.; Cooper, S. L. *Polyurethanes in Medicine*; CRC Press: Boca Raton, FL, 1986; p 57.
- (2) Ikada, Y. *Advances in Polymer Science*; Springer: Berlin, 1984; Vol. 57, p 103.
- (3) Grasel, T. G.; Cooper, S. L. *Biomaterials* **1986**, 7, 315.
- (4) Lelah, M. D.; Grasel, T. G.; Pierce, J. A.; Cooper, S. L. *J. Biomed. Mater. Res.* **1986**, 20, 433.
- (5) Gombotz, W. R.; Guanghui, W.; Horbett, T. A.; Hoffman, A. S. *J. Biomed. Mater. Res.* **1991**, 25, 1547.
- (6) Jeon, S. I.; Lee, L. H.; Andrade, J. D.; de Gennes, P.-G. *J. Colloid Interface Sci.* **1991**, 142, 149.
- (7) Munro, M. S.; Eberhart, R. C.; Maki, N. J. *Am. Soc. Artif. Intern. Organs J.* **1983**, 6, 65.
- (8) Pitt, W. G.; Grasel, T. G.; Cooper, S. L. *Biomaterials* **1988**, 9, 36.
- (9) Macroni, M.; Plozzi, A. *Macromol. Chem. Phys.* **1994**, 185, 875.
- (10) Jannasch, P. *Macromolecules* **1998**, 31, 1341.
- (11) Wen, J. M.; Somorjai, G.; Lim, F.; Ward, R. *Macromolecules* **1997**, 30, 7206.
- (12) Deslandes, Y.; Pleizier, G.; Alexander, D.; Santerre, P. *Polymer* **1998**, 39, 2361.
- (13) Zhang, D.; Gracias, D. H.; Ward, R.; Gauckler, M.; Tian, Y.; Shen, Y. R.; Somorjai, G. A. *J. Phys. Chem. B* **1998**, 102, 6225.
- (14) Desai, N. P.; Hubble, J. A. *Macromolecules* **1992**, 25, 226.
- (15) Desai, N. P.; Hubble, J. A. *Biomaterials* **1991**, 12, 144.
- (16) Bengt, W.; Maria, K.; Christina, F.-L.; Asa, L.; Marianne, P. *Biomaterials* **1994**, 15, 278.
- (17) Ohta, K.; Iwamoto, R. *Appl. Spectrosc.* **1985**, 39, 418.
- (18) Ohta, K.; Iwamoto, R. *Anal. Chem.* **1985**, 57, 2491.
- (19) Marco, C.; Fatou, J. G.; Gomez, M. A.; Tanaka, H.; Tonelli, A. E. *Macromolecules* **1990**, 23, 2183.
- (20) Coleman, M. M.; Lee, K. H.; Skrovanek, D. J.; Painter, P. C. *Macromolecules* **1986**, 19, 2149.
- (21) Harthcock, M. A. *Polymer* **1989**, 30, 1234.